Paper No: 040

19th National & 8th ISHMT-ASME
Heat and Mass Transfer Conference
January 3 - 5, 2008
JNTU Hyderabad, India

Analysis of Centrifugally Aided Micro-Capillary Filling and Related Interfacial Transport

Suman Chakraborty
Department of Mechanical Engineering
Indian Institute of Technology
Kharagpur-721302, INDIA
e-mail: suman@mech.iitkgp.ernet.in

Rajat Ghosh
Department of Mechanical Engineering,
Indian Institute of Technology,
Kharagpur-721302, India
Email: raj_iitkgp007@yahoo.co.in

Abstract

In this paper, a novel mathematical approach is devised to analyze the fluid flow through a rotating micro-channel. Special attention is devoted to estimate the effects of variable hydraulic resistance over different flow regimes and the dynamically evolving contact line forces. Flow characteristics depicting advancement of the fluid within the microfluidic channel turn out to be typically non-linear, as per the relative instantaneous strengths of the capillary forces, centrifugal forces and viscous resistances, evaluated in the rotating reference frame. The centrifugal forces are found to be clearly dominating during the later transients, especially for higher rotational speeds. It is revealed that excellent cooling performances can also be obtained by exploiting these features, for CD-based microchannel heat sinks.

1. Introduction

The recent advent of CD-based microfluidics (lab-on-a-CD concept) has opened up the possibilities of implanting complicated bio-microfluidic arrangements on relatively inexpensive rotating platforms [1, and the cross references therein]. Besides being advantageous because of their versatility in handling a wide variety of sample types, the ability to gate the flow of liquids (non-mechanical valving), simple rotational motor requirements, economized fabrication methods, large ranges of flow rates attainable, and the possibility of performing simultaneous and identical fluidic operations make the CD an attractive platform for multiple parallel assays. The CD platform (including the designed circuitry embedded within the same), coupled with automated liquid reagent loading systems, indeed appears to be ideal for future commercial introduction of more compact and inexpensive lab-on-a-chip based bio-microfluidic systems. The technology developed by the optical disc industry can conveniently be utilized to image the CD at the micron resolution, and possible extensions to DVD will allow submicron-scale resolution, leading to the integration of fluidics and informatics on the same disc. Moreover, the materials of the CDs are execlently conducive to the standard and micro-fabrication techniques and are also extremely bio-compatible in nature [2].

A number of research investigations have been reported in the literature on several distinctive aspects of centrifugally-aided microchannel flows on CD-based platforms, leading to the common consensus that rotational effects induce an artificial gravity to pulselessly pump the fluid in the radial direction. The first detailed theoretical model on centrifugally-aided capillary filling was developed by Kim and Kwon [3]. However, surface tension effects were neglected for deriving the capillary dynamics in their study. In a somewhat different perspective, Ducrée et al. [4] and Brenner et al. [5] demonstrated the capabilities of the rotationally-aided microchannel flows in enhancing the extent of microfluidic mixing, as influenced by the Coriolis effects, typically for high rotational speeds. However, for analytical convenience, fully developed velocity profiles as well as statically-affixed contact angles were considered in their study. On the contrary, it is well known from the classical fluid dynamics that internal flows are typically associated with an entrance region of length L_1, followed by a fully developed regime of length L_2. In microscale liquid flows, a third regime also comes into play, as attributed to the domination of surface effects. This third regime (of length L_3, say), namely the meniscus traction regime, physically originates due to a possible deviation of the velocity profile from its macro-scale counterpart, on account of strong interplay of adhesion and cohesion forces. In reality, the presence of the different flow regimes [6] is solely dictated by the instantaneous axial

length of the capillary mensiscus (l, say), during its dynamical evolution. For cases in which $l<L_1+L_3$, , and the entrance region and the meniscus traction region interact directly, leading to the condition of $L_2=0$. Fluid dynamic influences of the meniscus traction regime might be further complicated by the fact that the velocity of liquid meniscus itself can be related to its surface energy. In simplistic terms, immediately after a layer of fluid molecules is adsorbed to the microchannel surface, the next set of fluid molecules can march more easily in the microchannel, giving rise to a dynamic evolution of the contact angle. Physically, since the points on the interfacial lines arrive at the contact line within a finite time span, one must pose an effective slip law that relieves a force singularity condition by ensuring that a finite force is necessary to move the contact lines of a fluid, irrespective of the notional acceptability of the no-slip boundary conditions at the channel walls. In order to ensure the physical consistency behind the underlying theoretical treatment, one needs to pose a dynamical constraint on the contact angle θ, as a function of velocity of the contact line. From fluid dynamics perspective, this departure of contact angle from its static equilibrium value is mainly due to viscous bending of the interface near the contact lines. From such physical considerations, it can readily be inferred that neglecting the dynamical evolution of the surface forces in analyzing centrifugally-aided microchannel flows offers only with an idealized paradigm that is far from being the physical reality, if not a mere impossibility. Despite this fact, the literature on centrifugal-force driven transient filling of microchannels and microcapillaries routinely presumes either a zero surface tension force [3] or a constant contact angle with fully developed velocity profiles, as a fundamental basis for the underlying mathematical analysis, if not as a scientific ritual that is seldom realizable in practice. As such, despite the significant advancements have been made in the areas of CD-based microfluidics and lab-on-a-chip technology in recent times, no attempts have yet been made in the literature in offering with a fundamental theoretical description of centrifugally-aided microchannel flows in presence of dynamically evolving surface tension effects. However, such analysis can act as a key towards more fundamental and detailed understanding of the working principles of some of the newly synthesized biomedical microdevices that are to be designed on CD-based platforms.

Aim of the present study is to develop a fundamental transport model for analyzing the physics of centrifugally-assisted capillary filling mechanisms for CD-based microfluidic applications. It is noteworthy to mention in this context that in addition to the driving surface tension forces, the radially-outward centrifugal forces offer aiding influences for accelerating the capillary front, resisted by the opposing viscous forces. The competing effects of the driving and the retarding forces effectively determine the displacement, velocity and acceleration characteristics of the capillary front, in a dynamically evolving manner. A comprehensive theoretical model is developed in the subsequent section to address these issues in details. The primary emphasis behind the concerned theoretical analysis is to elucidate the dynamics of centrifugally-assisted microchannel flows by appealing to fundamental fluid dynamic considerations, and at the same time restricting the analysis to well-suited semi-analytical frameworks, without resorting to more complicated full-scale numerical analysis. The basic aim here is to obtain an improved qualitative and quantitative insight regarding interplay of the significant physical parameters governing the capillary transport process, by employing a simplistic approach that is easily extendible to more involved and accurate computations for applied research work in the years to come. The fluid dynamic transport model is subsequently utilized to predict the heat transfer characteristics of the microfluidic system, which might act as a fundamental design guideline for centrifugally-actuated micro-scale thermo-fluidic systems.

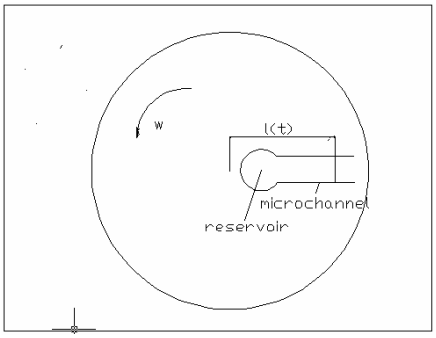

Figure 1: A schematic diagram depicting a microchannel on a rotating CD-base

2. Mathematical modeling

2.1 Description of the physical problem

As shown in fig. 1, fluid flow in a single representative microchannel is considered for theoretical analysis, which is fabricated on a circular substrate that can be actuated to rotate with designed angular velocities. An equivalent one-dimensional description of the capillary front advancement may be derived from the force balance considerations, by employing cross-sectionally-averaged quantities. The formulated governing equation essentially follows from a description of the Newton's second law of motion for a variable mass system in rotating reference frame. The fluid enters into the channel by the sole action of surface tension and advances further with an additional driving influence of the centrifugal effects. The fluid motion is opposed by the viscous resistances, as determined by the different flow regimes instantaneously prevailing within the capillary liquid.

For mathematical analysis of the above-mentioned physical situation, following major assumptions are made:

(a) The fluid flow is Newtonian and laminar.

(b) The width of the channel (w) is at least one order larger as compared to its height (h), so that a parallel plate channel with infinite transverse extent may be considered for theoretical analysis.
(c) At the entrance section of the channel, the motion of the fluid can be effectively modeled by a potential flow analysis, neglecting local dissipative effects.
(d) Coriolis effects are neglected for the ranges of rotational speeds considered in this study (it has been demonstrated by Kim and Kwon [3] that such assumptions are practically valid for rotational speeds less than 350 rad/s for flow of water through microchannels)
(e) The contact angle varies dynamically, as per prevailing flow conditions.

Under the above assumptions, the fluid flow is mathematically modeled by employing suitable governing equations and constitutive models, to be described subsequently.

2.2 The general governing equation of fluid motion

For a microchannel of depth H and width w, with instantaneous axial length (averaged over the cross section) occupied by the fluid as l, the governing equation of fluid motion can be described in a rotating reference frame in the following manner:

$$\frac{d}{dt}\left[\left(M_a+\rho Hlw\right)\frac{dl}{dt}\right]=P\sigma\cos\theta+F_C-F_D \qquad (1)$$

where ρ is density of the fluid, P is the wetted perimeter ($P=2(w+H)$), σ is the surface tension coefficient, θ is a dynamically evolving contact angle, F_C is the centrifugal force, and F_D is the viscous drag force. The centrifugal force can be estimated as

$$F_C=\int_0^l \omega^2 r\rho Hwdr=\frac{1}{2}\rho Hw\omega^2 l^2 \qquad (2)$$

where ω is the rotational speed. The viscous drag force can be theoretically calculated as

$$F_D=\int_0^l \tau_{xy}Pdx \qquad (3)$$

τ_{xy} being the pertinent shear stress component, x being the axial direction of flow and y being its orthogonal direction in the plane of flow. The term M_a in equation (1) is a so-called added mass, which accounts for the mass of the fluid droplet on the verge of entering the microcapillary channel. This can be mathematically modeled by drawing analogy from potential flow of a circular cylindrical lumped fluid mass of radius r_h, moving along the x-direction, where r_h is hydraulic radius of the channel, given by

$$r_h=\frac{2wH}{2(w+H)} \qquad (4)$$

It can be noted that following the work of Yih [7], the added mass M_a can be modeled as:

$$M_a=\rho\pi r_h^2 w/8 \qquad (5)$$

The physical consequence of this added mass can be appreciated by considering the case of initiation of flow (t=0, $l=0$), whereby one can encounter a situation of an infinitely large acceleration (refer to equation 1) at t=0, in case the contribution of M_a is not considered.

The mathematical model described as above is fairly general, and can lead to a well-posed problem, after specific models of the viscous and capillary effects are incorporated in equation (1). In the subsequent discussion, a development of those aspects is systematically attempted.

2.3 Modeling of the overall viscous drag

The net viscous drag force acting on the fluid can be thought of as a summation of drag forces offered in the entry regime, fully developed regime and the meniscus traction regime. Out of these three regimes, the flow resistance (per unit width) in the fully developed regime can be analytically derived in a straightforward manner, as [8]

$$\frac{dF_D^*}{dx}=\frac{12\mu\bar{u}}{H} \qquad (6)$$

where $\bar{u}$ is the fully developed average flow velocity. However, in reality, there are additional resistances due to the presence of entrance and the surface traction regimes, which cannot be analytically modeled. Nevertheless, experimental and/or full-scale computational results reported in literature in this regard can be utilized to a good effect for specification of this enhanced resistance. For example, for the entrance regime, the numerical work of Lew and Fung [9] can be effectively utilized to express the net drag force gradient ($\frac{dF_D}{dx}$) as

$$\frac{dF_D}{dx}=\left[1+f\left(\frac{x}{r_h}\right)\right]\frac{dF_D^*}{dx} \qquad (7)$$

where the function $f\left(\frac{x}{r_h}\right)$ takes care of the enhanced flow resistance in the entry region, details of which can be found in Lew and Fung [9], and are omitted here for the sake of brevity.

It is important to mention here that in addition to the viscous force being evaluated on the basis of a fully developed velocity profile in a parallel plate channel (in conjunction with the Newton's law of viscosity) mentioned as above, another frictional influence originates from the consideration that the microscopic contact angle may itself depend on the capillary flow velocity [10]. This can give rise to an additional velocity dependent frictional force, $F_D\big|_{\text{additioinal}}$. The source of this frictional force is the excitation of damped capillary waves at the liquid-vapour interface due the contact line motions over the wall roughness elements. From experimentally obtained data, this can be modeled approximately in the following form [10]:

$$F_D\big|_{\text{additioinal}} = 2\sigma\left(w+h\right)BCa^{x} \qquad (8)$$

where B and x are experimentally fitted constants, and $Ca=\frac{\mu u}{\sigma}$ is the capillary number. In the present study, various parameters pertinent to the specific slip model adopted are taken as follows [10] : K = 0.3, l_d = 5000 Å, B = 2.5, x = 0.3. A physical basis of the introduction of the additional frictional force can be provided by noting that the contact line jumps across the indentations on the solid boundaries, as the contact line moves forward. During the jump, the liquid-vapour interface is pulled forward by the interfacial tension and is retarded by the liquid viscosity. The jump speed is therefore of the order of $\frac{\sigma}{\mu}$, i.e., it conforms to Ca~1. Because of the restoring effects, the liquid-vapour interface actually executes a time-periodic motion on a local scale. Further, the contact line actually slips during the jump process, and the corresponding dissipative effects associated with this jump are responsible for the additional frictional force, which gives rise to a velocity dependent microscopic contact angle. One potential slip scenario is that the contact line actually leaves the solid surface on one side of the indentation and reattaches itself on the other side of the indentation, since, without that detachment, the large viscous stress near the contact line would retard the movement significantly, so that local jump speeds with Ca~1 would not be realizable.

2.4 Modeling of dynamic evolution of the contact angle

A second possible consequence of the contact line jump mechanism in the onset of capillary slip phenomenon. As per this mechanism, the contact line jumps across the indentations on the rough surfaces, while moving along the solid boundary, leading to a dynamical evolution of the contact angle, which can be estimated through the following functional dependence [11]:

$$G\left(\theta\right) = G\left(\theta_0\right) + Ca\,ln\left(\frac{K}{l_d}\right) + Ca\,ln\,Ca \qquad (9)$$

Here θ_0 is the microscopic contact angle, K is a slipping model dependent constant [11] , l_d denotes the scale of wall roughness and G(θ) is defined as [11]

$$G\left(\theta\right) = \int_0^{\theta}\left[f\left(\phi\right)\right]^{-1}\,d\phi \qquad (9a)$$

where

$$f\left(\phi\right) = \frac{2\sin\phi\left\{q^2\left(\phi^2-\sin^2\phi\right)+2q\left[\phi\left(\pi-\phi\right)+\sin^2\phi\right]+\left(\pi-\phi\right)^2-\sin^2\phi\right\}}{q\left(\phi^2-\sin^2\phi\right)\left[\left(\pi-\phi\right)+\sin\phi\cos\phi\right]+\left(\phi-\sin\phi\cos\phi\right)\left[\left(\pi-\phi\right)^2-\sin^2\phi\right]} \qquad (9b)$$

where q is the viscosity ratio of the two fluids forming the capillary. Despite its theoretical rigor, the above-mentioned expressions are mathematically somewhat involved in nature, in terms offering a direct physical basis of the dynamic evolution of the apparent contact angle. In an effort to elucidate the underlying consequences, one might refer to the reported experimental studies [12], which have revealed that the apparent dynamic contact angle that the liquid forms with the solid surface is closely described by a universal scaling relationship at low speeds, known as the Tanner's law, given as

$$\theta \sim Ca^{1/3} \qquad (10)$$

It is possible to utilize this scaling estimate as a starting basis, and perform an asymptotic analysis based on the thin liquid film in vicinity of the microchannel wall, close to the meniscus front. This thin film region can further be sub-divided into two parts, namely, (a) a lubricating film region followed by (b) a precursor film region as one moves along the direction of wetting. In the precursor film region, one expects the interfacial length scales to approach molecular scales, as intermolecular forces become important [13]. Behind the lubricating film, on the other hand, the length scales are quite large (of the order of r_h), and a potential challenge remains in devising a quantitative expression for dynamic evolution of θ by asymptotic matching from solutions to these regions of widely different length scales. For analysis of the same, one may assume negligible gravitational effects (typically characterized by a low Bond number, $Bo=\frac{\rho g r_h^2}{\sigma}$), and viscosity of the gas phase negligible in comparison to that of the liquid phase so that dynamics of the two phases are essentially decoupled. In that situation, the domain of interest can be divided into two regions, namely (i) the outer region where the lateral and vertical length scales are both O(1) and (ii) the inner lubrication region in which the lateral and vertical length scales are O($Ca^{1/3}$) and O($Ca^{2/3}$), respectively, as capillary and viscous forces balance [14-15]. Further division of the inner region may be necessary when the intermolecular forces become important at very thin films. In the lubricating film region, this effect can be incorporated by invoking an extra term of the same dimension as that of pressure in the overall force balance, which can be described as $A/6\pi z^3$, z being the film thickness. This term is known as the 'disjoining pressure'. The parameter A is called the Hamaker's constant [16], which is negative for wetting fluids. It needs to be noted here that one needs to be extremely careful in introducing intermolecular forces into a continuum model such as the Navier Stokes equation. In particular, the surface tension force, which is due to intermolecular forces between the gas and liquid phases, cannot be considered separately from the Van der Waals forces between the gas and the solid phases for very thin films. If one introduces a molecular length scale R_m as $R_m=\left(|A|/6\pi\sigma\right)^{1/2}$, or its

dimensionless counterpart $\lambda = R_m / r_h$; the above-mentioned model for lubricating film is valid if its film thickness is much larger than R_m, i.e., $Ca^{2/3} >> \lambda$. Since R_m is typically of the order of a few Angstroms, while a typically capillary radius is of the order of 10^{-1} mm, the lower bound on Ca is of the order of 10^{-4}. Beyond this lower bound, the continuum model remains valid for the lubricating film. At relatively larger Ca, the intermolecular forces would turn out to be less effective, so that dependence of Tanner's law on λ becomes progressively weaker. For a significantly large Ca, the meniscus speed may exceed the wetting speed and the meniscus may reverse its curvature as the contact angle passes through 90˚. However, the foregoing analysis assumes that such situations do not occur, and accordingly, it remains valid for θ<90˚. An asymptotic matching may accordingly be done between the outer region and the precursor film through the lubricating film at the inner region. At the front of this region, however, intermolecular forces and a vanishingly small film (spread by fast wetting) stipulate a hyperbolic decay of the film thickness towards zero. Accordingly, a universal relationship for dynamic evolution of the contact angle can be obtained as [17]

$$|\tan\theta| = 7.48 Ca^{1/3} - 3.28 \lambda^{0.04} Ca^{0.293} \qquad (11)$$

2.5 Heat transfer characteristics

The rotary microchannel, discussed as above, can also be conceptually utilized as an efficient cooling device. In order to make a preliminary assessment in this regard, one may consider the microchannel substrate to be subjected to a constant temperature, T_h, which is higher than the initial bulk mean flow temperature, T_c. Under these conditions, one can describe the transient evolution of the bulk mean flow temperature as

$$\frac{T - T_h}{T_c - T_h} = exp\left[-\frac{Pht}{\rho C_p A} \right] \qquad (12)$$

where C_p is the specific heat of the fluid, A is the microchannel cross sectional area, P is its perimeter, and h is the convective heat transfer coefficient. The consequent rate of heat transfer can accordingly be obtained as

$$\dot{Q} = \rho C_p A (T_h - T_c) \frac{dl}{dt} \left(1 - exp\left[-\frac{Pht}{\rho C_p A} \right] \right) \qquad (13)$$

3. Results and discussions

Eq. (1), coupled with eqs. (2, 3, 5, 7, 8, 11) is numerically solved after converting the same into a coupled set of first order initial value problems, using the 4th order Runge Kutta method. Physical properties and problem data, pertinent to the present simulation, are listed in table I.

TableI: Problem data

Microchannel height (h)	200 μm
Fluid density (ρ)	1000 kg/m^3
Surface tension coefficient (σ)	0.07 N/m
Static contact angle	0
Hamaker's constant (A)	-10^{-19} J
Viscosity	0.001 Pa.s

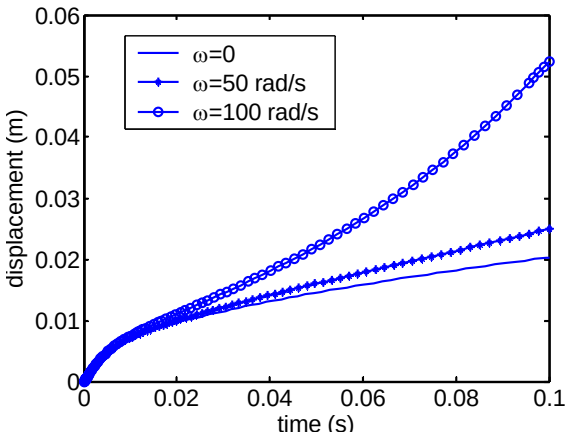

Figure 2: Time course of displacement of fluid into the channel.

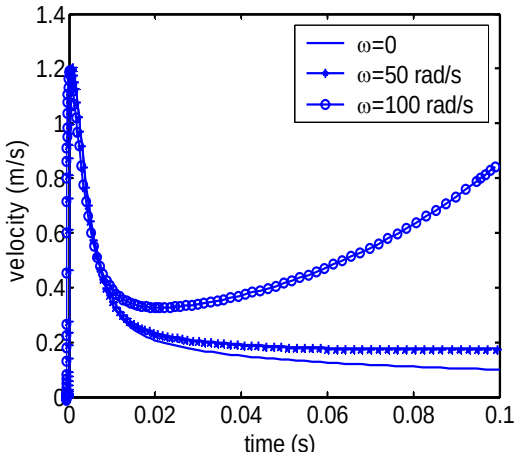

Figure 3: Time course of velocity of fluid into the channel.

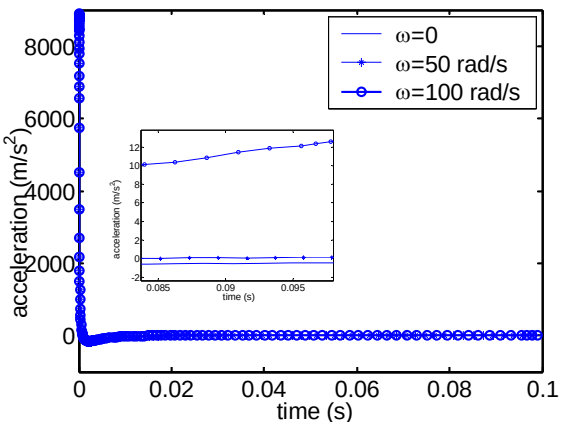

Figure 4: Time course of acceleration fluid into the channel.

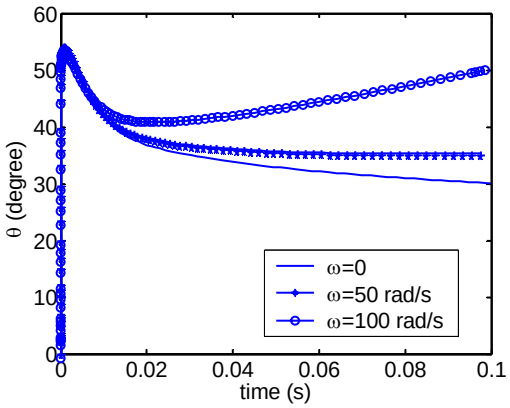

Figure 5: Variation of apparent contact angle with time.

Fig. 2 depicts advancement of the meniscus in the microchannel, as a function of time, for different values of the rotational speed. Interestingly, the displacement profile passes through an inflection point for ω =100 rad/s, which is not apparent at lower rotational speeds. This can be attributed to the fact that as the flow enters the microchannel, the viscous forces tend to slow down the capillary advancement speed substantially. In the absence of perceptible centrifugal effects, the capillary advancement can be sustained only with the aiding influences of the surface tension forces. These two forces, at some point of time, tend to come to a dynamical equilibrium, giving rise to an asymptotic nature of the velocity profile, although with a continuously decreasing velocity in the absence of strong centrifugal influences (see Fig. 3). However, with higher rotational speeds, the favorable influences of centrifugal forces appear to play a dominating role beyond the inflection point in the displacement profile, leading to a bifurcation of the displacement characteristics for different rotational speeds beyond that point. As time progresses, the capillary front marches further forward, and the centrifugal effects tend to become more and more dominating. This is in accordance with the dependence of the centrifugal influences on the square of the instantaneous position of the capillary meniscus. In the absence or weaker presence of centrifugal influences, however, the velocity decreases continuously (see Fig. 3), which may be attributed to the irreversible conversion of mechanical energy to unwanted thermal (internal) energy due to viscous effects and loss of energy via heat transfer. However, the velocity gets somewhat stabilized, as the driving capillary force becomes just sufficient to overcome a substantial proportion of the viscous resistances [18]. Despite such favorable influences of the surface tension forces, it still becomes impossible to have a recovery of higher flow velocities without the centrifugal influences. The acceleration characteristics of the meniscus (see Fig. 4), however, tend to exhibit an identical 'steadiness' at later instants of time, irrespective of the rotational speeds. There is a slight negative acceleration towards the end of the brief initial transients, due to dominance of resistance forces over accelerating forces in the developing region. However, as the flow becomes fully developed, and subsequently enters the meniscus traction regime, the net effective viscous drag decreases, and the capillary force is strong enough to overcome that in order to drive the fluid at nearly constant velocity, especially towards the later transients. Enhancements in velocities beyond these temporal regimes appear to be virtually impossible, without the progressively aiding influences of the driving centrifugal forces. The acceleration characteristics captured over the entire transience, however, cannot exhibit such effects quite emphatically, since this later recovery of acceleration is only a small proportion of the initial sharp decrement in the same. A magnification of the acceleration characteristics towards the later transients clearly manifests this effect, as demonstrated in the inset of Fig. 4.

Fig. 5 depicts the effect of a 'dynamic contact angle', as the fluid propagates inside the channel. Since velocity decreases sharply towards the end of the brief initial transience (immediately after the fluid is 'sucked' in), the Capillary number also decreases in accordance with the same, and consequently, the apparent contact angle decreases. Since the surface tension force is proportional to the cosine of this contact angle, it increases progressively as the contact angle decreases, during in-flow process of the fluid. This, in turn, implies a stronger driving force against the viscous drag. As the centrifugal force takes over, it tends to increase the capillary front speed over its dominating regime. This gives rise to a subsequent increment in the apparent contact angle for higher rotational speeds, giving rise to a relatively weaker aiding influence of the surface tension forces towards the later transients. The variation of the apparent contact angle, over the entire temporal evolution of the capillary advancement, is therefore by no means trivial. As such, significant errors can be incurred if the contact angle is assumed to remain a constant during the transients, at a value governed by a hypothetical static equilibrium consideration.

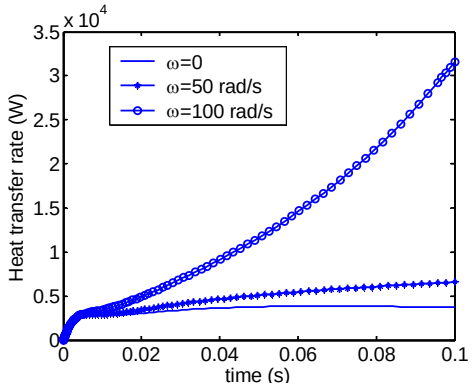

Fig. 6: Heat transfer rate across the capillary (expressed per unit cross sectional area), as a function of time

Fig. 6 depicts the rate of heat transfer (per unit cross sectional area of the microchannel) as a function of time, with C_p = 4.2kJ/kg. K, and $T_h - T_c$ =50°C. It is clearly evident from the figure that the centrifugally-assisted higher values of d*l*/d*t* for higher rotational speeds are responsible for better cooling performances, especially towards the later transients.

4. Conclusions

A detailed analysis of the influence of dynamically-evolving contact angles on the centrifugally-aided filling of microchannels has been undertaken in this study. From the fundamental physical insights developed in this study, improved design efforts for CD-based microfluidic systems can be made, by selecting judicious combinations of the fluid properties (density, viscosity, surface tension), microfluidic system dimensions (rotating substrate radius and the microchannel length), and the rotational characteristics (angular velocity), so as to obtain optimal capillary-filling characteristics, within the technological constraints of the chosen configuration.

From the present study, following major conclusions can be drawn:

1. The displacement characteristics of the capillary front are marked with a perceptible inflection point in presence of perceptible rotational influences, marking the onset of a centrifugally-dominated transient regime.
2. Influence of capillary forces dynamically evolves with time, based on the instantaneous relative dominance of the aiding or opposing forces. Since the contact angle reduces progressively with a reduction in the flow velocity, a consequent increase in the capillary force (which is proportional to cosine of the contact angle) takes place. On the other hand, the capillary forces tend to weaken progressively in case the contact line undergoes a positive acceleration.
3. The centrifugal effects tend to enhance the cooling rates for cases in which the CD-based platform is designed to operate as a microchannel heat sink.

References

1. M. Madou, J. Zoval, G. Jia, H. Kido, J. Kim, N. Kim, Lab on a CD, Annual Review of Biomedical Engineering **8**, 601-628, 2006.
2. Y-K Cho, J-G Lee, J-M Park, B-S Lee, Y. Lee, C. Ko, One-step pathogen specific DNA extraction from whole blood on a centrifugal microfluidic device, Lab on a Chip **7**, 565-573, 2007.
3. D. S. Kim, T. H. Kwon, Modeling, analysis, and design of centrifugal force driven transient filling flow into a circular microchannel, Microfluidics and Nanofluidics, DOI 10.1007/s10404-005-0053-8, 2005.
4. J. Ducrée, S. Haeberle, T. Brenner, T. Glatzel, R. Zengerle, Patterning of flow and mixing in rotating radial microchannels, Microfluidics and Nanofluidics, DOI 10.1007/s10404-005-0049-4, 2005.
5. T. Brenner, T. Glatzel, R. Zengerle, J. Ducrée, Frequency-dependent transversal flow control in centrifugal microfluidics, Lab on a Chip **5**, 146-150, 2005.
6. W. Huang, R. S. Bhullar, Y. C.Fung, The surface-tension-driven flow of blood from a droplet into a capillary tube, ASME Journal of Biomechanical Engineering **123**, 446-454, 2001.
7. C. S. Yih, Kinetic-energy mass, momentum mass, and drift mass in steady irrotational subsonic flow, J. Fluid Mech., **297**, 29–36, 1995.
8. F. M. White, Fluid Mechanics, McGrawHill, New York, 2003.
9. H. S. Lew and Y. C. Fung, Entry Flow Into Blood Vessels at Arbitrary Reynolds Number, J. Biomech. **3**, 23-28, 1970.
10. S. Chakraborty, R. Mittal, Droplet dynamics in a microchannel subjected to electrocapillary actuation, Journal of Applied Physics **101**, 104901, 2007.
11. P. Sheng, M. Zhou, Immiscible-fluid displacement: contact-line dynamics and the velocity-dependent capillary pressure, Physical Review A **45**, 5694-5708, 1992.
12. R. L. Hoffman, A study of the advancing interface I. Interface shape in liquid-gas systems J. Colloid Interface Sci. **50**, 228-235, 1975.
13. J. A. Nieminen, D. B. Abraham, M. Karttunen and K. Kaski, Molecular dynamics of a microscopic droplet on solid surface, Phys. Rev. Lett. **69**, 124-127, 1992.
14. F. P. Bretherton, The motion of long bubbles in tubes, J. Fluid Mech. **10**, 166-188, 1961.
15. C. W. Park and G. M. Homsy, Two-phase displacement in Hele Shaw cells: theory J. Fluid Mech. **139**, 291-308, 1984.
16. J. Israelachvili, Intermolecular Surface Forces, Academic Press, New York, 1992.
17. S. Kalliadasis and H-C Chang, Apparent dynamic contact angle of an advancing gas-liquid meniscus, Phys. Fluids. **6**, 12-23, 1994.
18. S. Chakraborty, Dynamics of capillary flow of blood into a microfluidic channel, Lab on a Chip **5**, 521-530, 2005.